



## $\sigma_8$ Discrepancy and its solutions

SUBHENDRA MOHANTY<sup>1,\*</sup>, SAMPURN ANAND<sup>1</sup>, PRAKRUT CHAUBAL<sup>1</sup>,  
ARINDAM MAZUMDAR<sup>1</sup> and PRIYANK PARASHARI<sup>1,2</sup>

<sup>1</sup>Physical Research Laboratory, Navrangpura, Ahmedabad 380 009, India.

<sup>2</sup>Indian Institute of Technology Gandhinagar, Gandhinagar 382 355, India.

\*Corresponding author. E-mail: mohanty@prl.res.in

MS received 8 June 2018; accepted 23 July 2018; published online 22 August 2018

**Abstract.** In the recent past, measurements of  $\sigma_8$  from large scale structure observations have shown some discordance with its value obtained from Planck CMB within the  $\Lambda$ CDM frame. This discordance naturally leads to a mismatch in the value of  $H_0$  also. Under the presumption that these discordances are not due to systematics, several attempts have been made to ameliorate the tensions. In this article, we describe the methods of determination of  $\sigma_8$  from large scale as well as CMB observations. We discuss that these discrepancies vanish if we consider the energy momentum tensor for an imperfect fluid which could arise due to self-interaction of dark matter or in an effective description of large scale structure. We demonstrate how the presence of viscosities in cold dark fluid on large scales ameliorate the problem elegantly than other solutions. We also estimate the neutrino mass in the viscous cosmological setup.

**Keywords.** CMB—large scale structure—viscosity—neutrino mass.

### 1. Introduction

In the past few decades or so, it has been established that our Universe, at today's epoch, is dominated by the dark components, i.e. dark matter and dark energy (Zwicky 1993; Rubin & Ford 1970; Perlmutter *et al.* 1997, 1999; Riess *et al.* 1998; Hinshaw *et al.* 2013; Ade *et al.* 2016a, b; Troxel *et al.* 2017). Most plausible theoretical construct, as of now, to understand the evolution of our Universe is provided by the so-called  $\Lambda$ CDM model. Most of the predictions of  $\Lambda$ CDM model are in agreement with Cosmic Microwave Background (CMB) and Large Scale Structure (LSS) observations. However some conflicts between these two observations, within the  $\Lambda$ CDM paradigm, have been consistently reported in the literature. To be specific, the value of  $\sigma_8$ , the rms fluctuation of perturbation  $8 h^{-1}$  Mpc scale, and the value of Hubble constant today  $H_0$  inferred from the CMB and LSS experiments are not in agreement with each other (Troxel *et al.* 2017; Vikhlinin 2009; Macaulay *et al.* 2013; Battye *et al.* 2015; MacCrann *et al.* 2015; Aylor *et al.* 2017; Raveri 2016; Lin & Ishak 2017; Abbott *et al.* 2017).

Several attempts have been made to address these discordances between CMB and LSS observations. A

list of attempts include the interaction between dark matter and dark energy (Pourtsidou & Tram 2016; Salvatelli *et al.* 2014; Yang & Xu 2014), interaction between dark matter and dark radiation (Ko & Tang 2016, 2017; Ko *et al.* 2017), dynamical dark energy model (Park & Ratra 2018; Lambiase *et al.* 2018) as well as modification in the neutrino sector (Wyman *et al.* 2014; Battye & Moss 2014; Riemer-Sørensen *et al.* 2014). However, these attempts fail to resolve both the conflicts simultaneously. In this work, we show that if we incorporate the dissipative effects in the energy momentum tensor describing the energy content of the Universe, the two discordances can be ameliorated simultaneously.

It has been discussed that the dissipative effect, characterized by the coefficient of viscosity, in CDM has the ability to reduce the power on small length scales which leads to suppression in the matter power spectrum on those length scales (Blas *et al.* 2015; Velten *et al.* 2014; Thomas *et al.* 2016). Attempts to quantify the dissipative effects in dark matter have been done in Kunz *et al.* (2016) from Baryon Acoustic Oscillation (BAO) data. For a recent review on this topic, we refer to Brevik *et al.* (2017) and references therein. There are two different kinds of viscosities: bulk and shear

viscosities. The bulk viscosity suppresses the growth of structures by imparting a negative pressure against the gravitational collapse while the shear viscosity reduces the amount of velocity perturbations which in turn stops the growth. Another distinction between bulk and shear viscosity is that the former acts homogeneously and isotropically while the latter breaks these symmetries. Therefore, on small length scales, where the homogeneity and isotropy are broken due to velocity gradients, effects of shear viscosity are expected to play a crucial role. Although the physics of these viscosities are different, we will show that their effect on large scale structure is more or less similar.

Massive neutrinos also suppress the power on small length scales, but they fail to resolve the two discordances simultaneously. But viscous paradigm does explain them. Therefore, we consider the viscous cold dark matter along massive neutrinos to constrain neutrino mass and comment on the neutrino mass hierarchy.

This article is structured as follows: We start by reviewing the concept of halo mass function and quantity of central importance for our discussion,  $\sigma_8$ , in section 2. We then describe the tensions between the Planck CMB and LSS observation as well as previous attempts made to ease the tensions in section 3. Thereafter, we move on to discuss the viscous paradigm in section 4 and discuss about the origin of cosmic viscosities. We write down the cosmological perturbation equation in viscous setup in section 5. Finally, we present the results in section 6 and conclude in section 7.

## 2. Halo mass function and $\sigma_8$

Linear perturbation theory works perfectly well during the period of CMB. It is because the density perturbations are of the order of  $10^{-3}$  in CDM and  $10^{-5}$  for the baryonic matter. All the perturbations remain in the linear regime in this epoch. But around redshift  $z = 50$ , CDM perturbations start growing above one which makes the non-linear growth more important. Finally the large scale structures that we see today, completely get generated in a non-linear process.

Although the collapse process is non-linear, at late time, the number density of virialized objects can be linked with the linear perturbation theory through the halo mass function. The halo mass function is defined as

$$\frac{dN}{dM} = n(M). \quad (1)$$

The first type of halo mass function was proposed by [Press and Schechter \(1974\)](#) which assumes that the

initial distribution of over-densities is Gaussian in nature. Moreover, those over-densities which can reach a critical value  $\delta_c$ , if linearly extrapolated, are expected to form a virialized object. These two assumptions lead to a halo mass function which can be written as

$$n(M)dM = -\sqrt{\frac{2}{\pi}} \frac{d\sigma_M}{dM} \frac{\bar{\rho}}{M} \frac{\delta_c}{\sigma_M^2} \exp\left(\frac{-\delta_c^2}{2\sigma_M^2}\right) dM, \quad (2)$$

where  $\sigma_M$  is the standard deviation of the distribution calculated from linear matter power spectrum  $P(k)$  at a length scale

$$R = \left(\frac{3M}{4\pi\bar{\rho}}\right)^{1/3}. \quad (3)$$

The quantity  $\bar{\rho}$  is the background density at any epoch and the standard deviation  $\sigma_M$  is given as

$$\sigma_M = \frac{1}{2\pi^2} \int_{2\pi/R}^{\infty} dk k^2 P(k) |W(k, R)|^2 \quad (4)$$

with  $W(k, R)$  being the appropriate window function.

The halo mass function can be matched with  $N$ -body simulation which allows cold dark matter to interact gravitationally and simulates non-linear structure formation. Although the Press–Schechter mass function provided the basic shape of the halo mass function, it fails to match with simulation in the low and high  $M$  region. Therefore, more precise mass functions have been proposed by different authors and parameters of those mass functions are fitted from  $N$ -body simulations. Amongst these, the most common are the Sheth-Tormen mass function ([Sheth & Tormen 1999](#)) and the Tinker *et al.* mass function ([Tinker \*et al.\* 2008](#)). The mass function proposed by [Tinker \*et al.\* \(2008\)](#) is given by

$$\frac{dn(\sigma)}{d\sigma} = A \left[ \left(\frac{\sigma}{b}\right)^{-a} + 1 \right] e^{-c/\sigma^2} \quad (5)$$

The parameters  $A$ ,  $a$ ,  $b$  and  $c$  are dependant on  $z$  and their values are fitted from  $N$ -body simulation. Therefore, the mass function itself is a redshift-dependant quantity. The  $z$  dependence of  $\sigma_8(R = 8 h^{-1} \text{ Mpc})$  can be written as

$$\begin{aligned} \sigma_8(z) &= \frac{1}{2\pi^2} \int_{k_i}^{\infty} dk k^2 P(k, z) |W(k, R)|^2 \\ &= g(z) \frac{1}{2\pi^2} \int_{k_i}^{\infty} dk k^2 P(k, 0) |W(k, R)|^2, \end{aligned} \quad (6)$$

where  $k_i = 2\pi h/8 \text{ Mpc}$  and  $g(z)$  is the growth parameter which has to be normalized to 1 at  $z = 0$ . Moreover, the growth function can be parametrized in terms of  $\Omega_m(z)$  as

$$\sigma_8(z) = \left( \frac{\Omega_m(z)}{\Omega_m^0} \right)^\alpha \sigma_8^0. \quad (7)$$

Now any large scale observation gives its result in either of these two ways: number of halos at some particular  $z$  or the number of halos integrated over  $z$  (like SZ or lensing). Whatever be the type of result, once the other parameters of the mass function are determined from simulation, the unknown quantity to be determined is  $\sigma_8(z)$ . Therefore, there always exists a degeneracy between the growth and the primordial amplitude of  $P(k)$ , or equivalently, between  $\Omega_m^0$  and  $\sigma_8^0$ . In order to estimate parameters from the observations,  $\Omega_m^0$  in the denominator of equation (7) is generally taken as a reference value  $\Omega_{\text{ref}}$  and  $\Omega_m(z) = \Omega_m^0 (1+z)^3$ . Therefore equation (7) turns out to be

$$\sigma_8(z) = \underbrace{\left( \frac{\Omega_m^0}{\Omega_{\text{ref}}} \right)^\alpha}_{S_8} \sigma_8^0 \times (1+z)^{3\alpha}. \quad (8)$$

In case of  $z$  integrated observations, we get

$$S_8 = \left( \frac{\Omega_m^0}{\Omega_{\text{ref}}} \right)^\alpha \sigma_8^0 = \text{constant value}. \quad (9)$$

Therefore all the  $z$  integrated observations try to find some combination like equation (9) which are independent of  $\Omega_m^0$ . The value of  $\alpha$  varies from observation to observation and depends on the choice of mass function.

### 3. Discrepancies and earlier attempts to remove them

In the previous section, we have described how a relation between  $\sigma_8$  and  $\Omega_m^0$  is established by large scale observations. On the contrary, CMB observations determine the basic six cosmological parameters. Using these six cosmological parameters with linear perturbation theory, the value of  $\sigma_8^0$  can be calculated. Recently, it has been reported that there is a discordance between the values of  $\sigma_8$ , inferred from Planck-CMB data and that from LSS observations. In this section, we briefly discuss the tensions between CMB and LSS observations.

#### 3.1 Tension in $\sigma_8 - \Omega_m^0$ plane

The impact of lensing on the temperature power spectrum is quantified using the power spectrum of the lensing potential which is estimated from the lensing observations. The lensing potential depends on the amplitude of primordial perturbations  $A_s$  and the scale

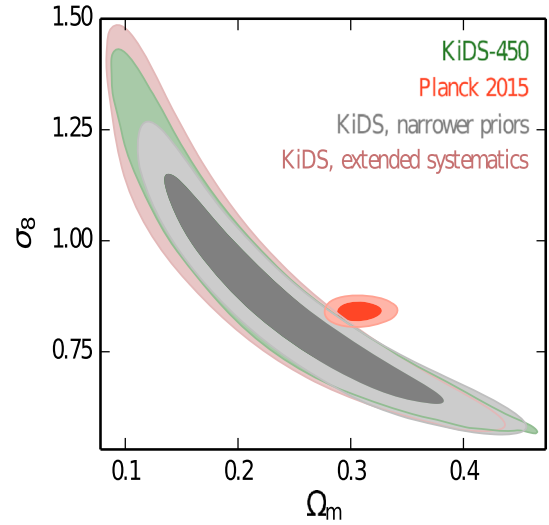


**Figure 1.** KiDS lensing result is shown in the green patch which follows the form of equation (9). The red area is the Planck CMB result. This plot is taken from [Joudaki et al. \(2017\)](#).

corresponding to the matter radiation equality,  $k_{\text{eq}}$  ([Pan et al. 2014](#); [Ade et al. 2016a, b](#)). The amplitude of the matter power spectrum changes with change in  $A_s$  while the turning point shifts when  $k_{\text{eq}}$  changes. Thus,  $A_s$  and  $\Omega_m$  determines the features of matter power spectrum. This effect get manifested in the lensing power spectrum as well. Moreover,  $\sigma_8$  is proportional to  $A_s$  and depends on  $\Omega_m$  through the growth factor.

In SZ surveys, what is measured is the number of clusters with the given mass in a given volume along the line-of-sight ([Ade et al. 2014a](#)). It is described as  $z$  integrated observation in the previous section.

The best-fit value of  $\Omega_m^0$  and  $A_s$  obtained from the CMB experiments gives a value of  $\sigma_8$  from the theoretically predicted matter power spectrum using  $\Lambda$ CDM cosmology. This value does not match with the  $\sigma_8 - \Omega_m^0$  degeneracy direction at  $2\text{-}\sigma$  level. This degeneracy has been mentioned in many experiments. As an example from the recent observations we show the KiDS result in Fig. 1 taken from ([Joudaki et al. 2017](#)). The joint analyses by combining different LSS experiments (as described in the Introduction) is shown in Fig. 2 taken from [Anand et al. \(2017\)](#).

#### 3.2 Tension in $H_0 - \Omega_m^0$ plane

The value of the Hubble parameter is determined in two ways: (a) directly, using supernova observations, and (b) indirectly using CMB and LSS observations. We highlight that we are addressing the discrepancy in the indirect observations only.

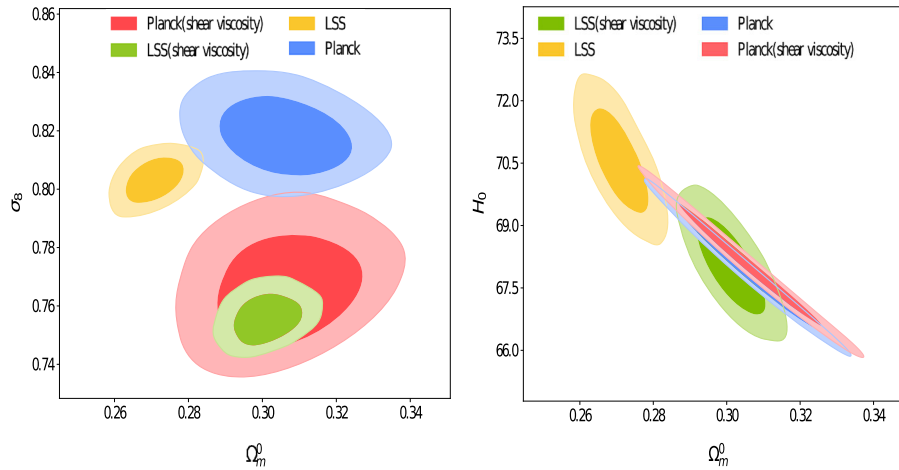


**Figure 2.** Tension in allowed values of  $\sigma_8$  and  $H_0$  inferred from Planck CMB and LSS (Planck SZ survey, [Ade et al. 2014a](#)), Planck lensing survey ([Ade et al. 2014b](#)), Baryon Acoustic Oscillation data from BOSS ([Anderson et al. 2013](#); [Font-Ribera et al. 2014](#)), South Pole Telescope (SPT) ([Schaffer et al. 2011](#); [Engelen 2012](#)) and CFHTLenS ([Kilbinger et al. 2013](#); [Heymans et al. 2013](#)) observations are shown. In the viscous framework, this mismatch in the allowed values of  $\sigma_8$  and  $H_0$  are resolved simultaneously.

Indirect measurement of Hubble parameter is done through the scale of baryon acoustic oscillation (BAO) at the last scattering surface,  $\theta_{MC}$ , which is actually inferred from CMB. Similarly, acoustic oscillation in the matter power spectrum is also observed by LSS surveys like SDSS. The comoving acoustic oscillation scale is considered as the standard ruler in cosmology and hence, we can determine the comoving distance from BAO ([Bassett and Hlozek 2009](#)). The comoving distance at a particular  $z$  is

$$\chi(z) = \int_0^z \frac{dz'}{H(z')}, \quad (10)$$

where

$$H(z)^2 = H_0^2 (\Omega_m^0 (1+z)^3 + \Omega_\Lambda). \quad (11)$$

Thus, one can estimate the value of  $H_0$  from BAO observations provided the value of  $\Omega_m^0$  is given. A joint analyses of LSS experiments give some best-fit value of  $\Omega_m^0$  rather than a large range. This  $\Omega_m^0$  is little less than the  $\Omega_m^0$  obtained from Planck CMB observations, which makes the value of  $H_0$  derived from LSS joint analysis little higher than that derived from Planck CMB observation as seen in Fig. 2.

### 3.3 Attempts to ease the tensions

Considerable efforts have been put to ease the discordance between CMB and LSS observations. It has been argued that the interaction between dark matter and dark energy ([Poursidou & Tram 2016](#); [Salvatelli et al. 2014](#); [Yang & Xu 2014](#)) as well as dark matter

and dark radiation ([Ko & Tang 2016, 2017](#); [Ko et al. 2017](#)) have the potential to resolve this tension to some extent. In most of the cases, such models resolve one of the above mentioned tensions but fail to solve the other one. More importantly, interaction between the dark sectors can also modify the scale corresponding to matter radiation equality ([Yang & Xu 2014](#)) which might introduce greater problem than the  $\sigma_8$  mismatch. Another approach adopted to address these issues is to modify the neutrino sector ([Wyman et al. 2014](#); [Battye & Moss 2014](#); [Riemer-Sørensen et al. 2014](#)). For instance, addition of massive sterile neutrino in the system has been reported to reduce tension in  $H_0 - \Omega_m^0$  plane to some extent but not in  $\sigma_8 - \Omega_m^0$  plane ([Wyman et al. 2014](#); [Battye & Moss 2014](#)).

We discuss the reason behind not solving the tension in detail. Whatever be the model of interest, the main purpose was to suppress the linear matter power spectrum so that the value of  $\sigma_8$  goes down. But this should happen without affecting other parameters. Let us take the example of massive neutrinos.

Massive neutrinos have an important property that they are relativistic in the early Universe and contribute to the radiation density while in the late time, when they turn non-relativistic, they contribute to the total matter density. The collision-less nature of the neutrinos, after they become non-relativistic, allow them to free-stream on scales  $k > k_{fs}$ , where  $k_{fs}$  is the wave number corresponding to the scale of neutrino free streaming. Hence, this will wash out the perturbations on length scales smaller than the characteristic scale  $k_{fs}$ . Thus massive neutrinos be it sterile or active suppresses matter power

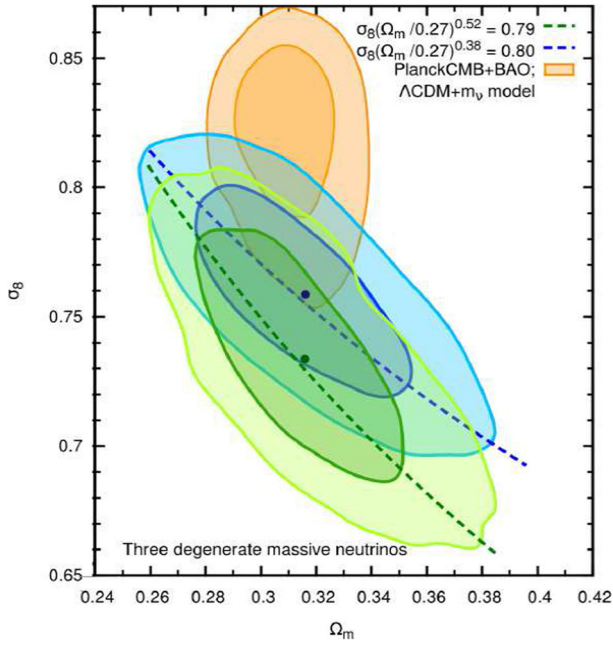


**Figure 3.** The red part shows  $\sigma_8$  from CMB, the blue region is the LSS result without modifying the mass function, and the green region is the LSS result after modifying the mass function. This plot is taken from Costanzi *et al.* (2013).

spectrum, but with a cost of increasing  $\Omega_m^0$ . Therefore massive neutrinos can resolve the  $H_0$  tension, but fails to resolve the  $\sigma_8$  problem. Since the inclusion of massive neutrinos resolve some tension in the parameter space, it leads to some improvement in  $\chi^2$ . However it has been argued that this improvement is most possibly an over-estimation of the effect of massive neutrinos (Costanzi *et al.* 2013). It is because, as we have described in the previous section, determination of  $S_8$  requires the halo mass function. Halo mass function is expected to change for inclusion of massive neutrinos. Therefore the value of  $S_8$  will also change. This will even worsen the situation and increase the tension in the  $\sigma_8 - \Omega_m^0$  plane. This has been shown in detail in Costanzi *et al.* (2013). Figure 3 shows the effect of massive neutrinos on the  $\sigma_8 - \Omega_m^0$  plane.

In the next section, we will show cosmic viscosities as the solution of the tension. We need to point out that similar problems like these are faced in the case of neutrinos and are expected to arise in the case of viscosity too. If the viscosities in CDM are of fundamental nature then we should perform  $N$  body simulation with viscous dark matter, derive the halo mass function and generate  $S_8$  from the observations. But viscosity is of effective nature and then we can get rid of that. The reason behind it will be evident in the next section when we describe different sort of viscosities. Moreover,

viscosity has one more benefit. Unlike massive neutrinos it does not change  $\Omega_m^0$ .

#### 4. Cosmic viscosity

Before we use the cosmic viscosity as a remedy for the above mentioned discrepancies, a small description about the origin of cosmic viscosity at this stage would be appropriate.

##### 4.1 Origin of viscosity

Depending on the origin of viscosities, they are classified into two classes:

- *Fundamental viscosity.* The diffusive transport of momentum by the constituents of the fluid can lead to viscosity. Such a viscosity is ultimately related to the fundamental interactions between the constituents of the fluid under consideration.
- *Effective viscosity.* The Universe is characterized by two well separated scales namely, the Hubble scale, over which perturbations are linear and the scale of non-linearity which is the scale over which gravitational collapse overtakes the expansion. These well separated scales make the study of large scale structure amenable to an effective field theory treatment. In this effective theory, the quasi linear modes of the perturbations evolve in the presence of an effective fluid whose properties are determined by non-linear short wavelength modes. To describe the coupling of UV-IR modes of cosmological fluctuations, we first decompose the Einstein tensor into (i) homogeneous background, (ii) terms that are linear and (iii) terms that are non-linear in metric perturbations, i.e.,

$$\bar{G}_{\mu\nu}(\bar{g}_{\mu\nu}) + (G_{\mu\nu}(\delta g_{\mu\nu}))^L + (G_{\mu\nu}(\delta g_{\mu\nu}^2))^{\text{NL}} = \kappa T_{\mu\nu}.$$

After re-organizing the Einstein equation by considering the background equation  $\bar{G}_{\mu\nu} = \kappa \bar{T}_{\mu\nu}$ , the linearized equations  $(G_{\mu\nu})^L = \kappa (T_{\mu\nu})^L$  are defined in the standard way. Thus, the non-linear Einstein equation can be written in the following form:

$$(G_{\mu\nu})^L = \kappa(\pi^{\mu\nu} - \bar{T}_{\mu\nu}), \quad (12)$$

where the effective stress energy pseudo-tensor is defined as

$$\pi^{\mu\nu} = T_{\mu\nu} - \frac{(G_{\mu\nu})^{\text{NL}}}{\kappa}. \quad (13)$$

This pseudo-tensor captures the dissipative effects.

## 5. Cosmological perturbation theory in viscous cosmology

In this section, we will discuss the perturbation theory for the CDM with viscosity and massive neutrinos. Since neutrinos do not interact among themselves in the standard picture, their mean-free path is infinite and we can not treat them as a fluid. Therefore, we will solve the Boltzmann equation to get the evolution equation for neutrino and derive perturbation equation for CDM using the conservation equation.

### 5.1 Cold dark matter

The energy momentum tensor for CDM with viscosity is given as (Weinberg 1972)

$$T_{\text{cdm}}^{\mu\nu} = \rho_{\text{cdm}} u^\mu u^\nu + (p + p_b) \Delta^{\mu\nu} + \pi^{\mu\nu}, \quad (14)$$

where  $\rho_{\text{cdm}}$  and  $p$  is the energy density and pressure of the CDM respectively.  $u^\mu$  and  $p_b = -\zeta \nabla_\mu u^\mu$  are respectively the fluid flow vector and the bulk pressure with the coefficient of bulk viscosity  $\zeta$ .  $\Delta^{\mu\nu} = u^\mu u^\nu + g^{\mu\nu}$  is the projection operator which projects the quantity on the three dimensional space like hypersurface and  $\pi^{\mu\nu}$  is the anisotropic stress tensor and is given by

$$\begin{aligned} \pi^{\mu\nu} &= -2\eta \sigma^{\mu\nu} \\ &= -2\eta \left[ \frac{1}{2} (\Delta^{\mu\alpha} \nabla_\alpha u^\nu + \Delta^{\nu\alpha} \nabla_\alpha u^\mu) \right. \\ &\quad \left. - \frac{1}{3} \Delta^{\mu\nu} (\nabla_\alpha u^\alpha) \right], \end{aligned} \quad (15)$$

where  $\eta$  is the coefficient of shear viscosity and  $\nabla$  denotes the covariant derivative compatible with the given metric which we will define later in this section. We treat baryonic matter as an ideal fluid.

Assuming the homogeneity and isotropy of the background, the perturbations can be decomposed into the background and the perturbed part. Since Einstein equation relates the perturbations in matter field to that in metric and vice-versa, we introduce the perturbations in FRW metric as

$$ds^2 = a^2(\tau) [-(1+2\psi) d\tau^2 + (1-2\phi) dx_i dx^i], \quad (16)$$

where  $\psi \equiv \psi(\tau, \vec{x})$  and  $\phi \equiv \phi(\tau, \vec{x})$  are space-time dependent perturbations. We also introduce the perturbations in the fluid flow  $u^\mu$  as

$$u^\mu = (1 - \psi, v^i), \quad (17)$$

which satisfies  $u^\mu u_\mu = -1$  in the first order limit of perturbations. The evolution equations for the

background fields are given by the Friedmann equation and continuity equation, which are given as

$$\mathcal{H}^2 = \left( \frac{\dot{a}}{a} \right)^2 = \frac{8\pi G}{3} (\rho_m + \Lambda) a^2, \quad (18)$$

$$\dot{\rho}_i + 3\mathcal{H}(\rho_i + p_i) = 0, \quad (19)$$

where  $\rho_m = \rho_b + \rho_{\text{cdm}} + \rho_\nu$  is the total matter density and  $\rho_i$  stands for each species. Here dot denotes the derivative with respect to the conformal time  $\tau$  and  $\mathcal{H}$  is the Hubble parameter. We get the evolution equation for the density and velocity perturbations from the perturbed part of the continuity equation (Anand *et al.* 2017, 2018)

$$\begin{aligned} \dot{\delta} &= - \left( 1 - \frac{\tilde{\zeta} a}{\Omega_{\text{cdm}} \tilde{\mathcal{H}}} \right) (\theta - 3\dot{\phi}) + \left( \frac{\tilde{\zeta} a}{\Omega_{\text{cdm}} \tilde{\mathcal{H}}} \right) \theta \\ &\quad - \left( \frac{3\mathcal{H}\tilde{\zeta}a}{\Omega_{\text{cdm}}} \right) \delta \end{aligned} \quad (20)$$

and

$$\begin{aligned} \dot{\theta} &= -\mathcal{H}\theta + k^2\psi - \frac{k^2 a \theta}{3\mathcal{H}(\Omega_{\text{cdm}} \tilde{\mathcal{H}} - \tilde{\zeta} a)} \left( \tilde{\zeta} + \frac{4\tilde{\eta}}{3} \right) \\ &\quad - 6\mathcal{H}\theta \left( 1 - \frac{\Omega_{\text{cdm}}}{4} \right) \left( \frac{\tilde{\zeta} a}{\Omega_{\text{cdm}} \tilde{\mathcal{H}}} \right), \end{aligned} \quad (21)$$

where  $\tilde{\eta} = \frac{8\pi G\eta}{\mathcal{H}_0}$  and  $\tilde{\zeta} = \frac{8\pi G\zeta}{\mathcal{H}_0}$  are the dimensionless parameters.

### 5.2 Massive neutrino

As discussed earlier, we will solve Boltzmann equation for massive neutrino to get the evolution equation for density and velocity perturbations. The energy momentum tensor for massive neutrinos is given in terms of distribution function. To write the perturbation equations for neutrino, we expand the distribution function  $f(x^i, P_j, \tau)$  around zeroth-order distribution function  $f_0$ . The zeroth-order terms of  $T_{\mu\nu}$  gives the unperturbed energy density and pressure of massive neutrinos which reads as

$$\begin{aligned} \bar{\rho} &= 4\pi a^{-4} \int q^2 dq \epsilon f_0(q), \\ \bar{P} &= \frac{4\pi a^{-4}}{3} \int q^2 dq \frac{q^2}{\epsilon} f_0(q), \end{aligned} \quad (22)$$

where  $\epsilon = \epsilon(q, \tau) = \sqrt{q^2 + m_\nu^2 a^2}$ . Since  $\epsilon$  is dependant on both momentum and time, we can not directly integrate out the momentum dependence. Therefore we expand the perturbation in the distribution function in

the Legendre series and use the series expansion to get the the perturbed energy density, pressure, energy flux and shear stress for the massive neutrinos (Ma & Bertschinger 1995). Boltzmann equations for different moments of distribution function take the following forms in conformal Newtonian gauge:

$$\begin{aligned} \dot{\Psi}_0 &= -\frac{qk}{\epsilon}\Psi_1 - \dot{\phi} \frac{d \ln f_0}{d \ln q}, \\ \dot{\Psi}_1 &= \frac{qk}{3\epsilon}(\Psi_0 - 2\Psi_2) - \frac{\epsilon k}{3q}\psi \frac{d \ln f_0}{d \ln q}, \\ \dot{\Psi}_l &= \frac{qk}{(2l+1)\epsilon}[l\Psi_{l-1} - (l+1)\Psi_{l+1}] \quad \forall l \geq 2. \end{aligned} \quad (23)$$

### 5.3 Effects on matter power spectrum

The perturbation equations obtained in the previous section is passed to the CLASS code (Blas *et al.* 2011; Lesgourgues & Tram 2011) to obtain the matter power spectrum  $P(k)$  which is shown in Fig. 4 which is taken from Anand *et al.* (2018). It is clear from Fig. 4 that both viscosity and massive neutrinos have a similar effect on the matter power spectrum. The effective viscosity reduces the growth of density perturbations  $\delta$  which in turn effects the matter power spectrum. It is important to note that the perturbation equations contain terms in which viscosity coefficient always comes with  $k$  which, therefore implies that the viscous effects are more prominent on large  $k$  or small length scales. Hence, the effective viscosity suppresses the power on large  $k$  scales (see Fig. 4). Also the effect of both shear

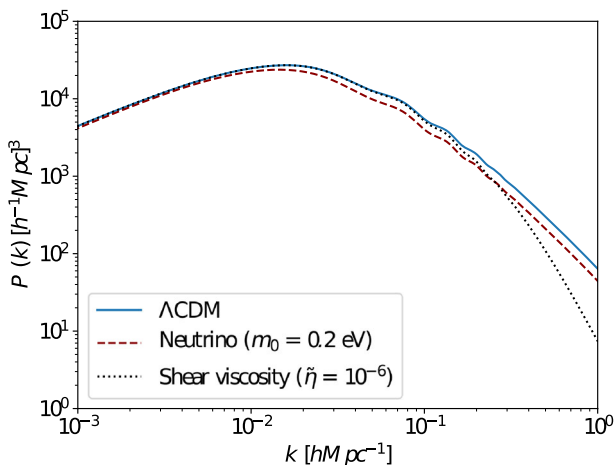


**Figure 4.** Both viscosity and neutrino suppress the matter power spectrum. Viscosity suppresses  $P(k)$  strongly on small length scales, whereas the effect of neutrinos is visible on scales greater than  $k_{nr}$ .

and bulk viscosities are similar in nature, therefore we use only shear viscosity for further analysis.

It has already been pointed out that neutrinos also affect  $P(k)$  in a similar manner as viscosity does. The massive neutrinos have this important property that they stream freely on scales greater than the scale corresponding to the free streaming length of neutrinos, i.e,  $k > k_{fs}$ . In general  $k_{fs}$  depends on  $z$  and attain the minimum value  $k_{nr}$ . The  $k_{nr}$  is a mass dependant quantity and is defined as the scale which re-enter the horizon at the time when neutrino turns non-relativistic. It is given as

$$k_{nr} = 0.018 (\Omega_m^0)^{1/2} \left( \frac{m_i}{1 \text{ eV}} \right)^{1/2} h \text{ Mpc}^{-1}. \quad (24)$$

Hence, perturbations on the scales  $k > k_{nr}$  stream out of the high density regions and do not form a structure. On the other hand, perturbations on the scales  $k < k_{nr}$  behave as CDM and are washed out on these scales. Therefore, massive neutrino suppresses the power on the small length scales. This effect can be seen clearly in the matter power spectrum (see Fig. 4).

## 6. Results

We have done MCMC analysis using MontePython (Audren *et al.* 2013) of Planck and LSS data. Here we refer Planck-CMB observations (Ade *et al.* 2016a,b) as Planck data, whereas LSS data includes data from Planck SZ survey (Ade *et al.* 2014a), Planck lensing survey (Ade *et al.* 2014b), Baryon Acoustic Oscillation data from BOSS (Anderson *et al.* 2013; Font-Ribera *et al.* 2014), South Pole Telescope (SPT) (Schaffer *et al.* 2011; Engelen 2012) and CFHTLenS (Kilbinger *et al.* 2013; Heymans *et al.* 2013). First, we run MCMC analysis with Planck and LSS data separately with just six standard cosmological parameters and two derived parameters. We plot the two derived parameters  $\sigma_8$  and  $H_0$  against  $\Omega_m^0$  (see Fig. 2). It is clear from Fig. 2 that there is discordance between values obtained from Planck and LSS observations. Thereafter we run the MCMC analysis with viscous effect taken into account and found that the tension between the values of  $\sigma_8$  and  $H_0$  inferred from Planck and LSS observations has resolved simultaneously in the viscous framework (see Fig. 2).

### 6.1 Viscous cosmological parameters

We have already discussed that viscosity resolves the tension between Planck and LSS observations. In this subsection, we discuss the cosmological parameters

obtained from the analysis with Planck and LSS observations. We perform MCMC analysis of Planck and LSS combined data sets to find the best fit value of viscosity parameters. We have performed three analyses. In the first run, we kept both the viscosity parameters  $\tilde{\eta}$  and  $\tilde{\zeta}$  varying and obtained their best-fit values. In the next two runs, we kept either  $\tilde{\eta}$  or  $\tilde{\zeta}$  to be zero and obtained the best-fit values for the other parameters. All the best-fit values are listed in Table 1. From these analyses, we also found the best-fit values of six cosmological parameters and two derived parameters. We found that the value of derived parameter  $\sigma_8$  is less than the Planck-fitted value. There is no significant difference between the best-fit value of  $\sigma_8$  obtained from the analysis done with either  $\tilde{\eta}$  or  $\tilde{\zeta}$  to be zero and that of the analysis done with both the viscosity

parameters. We also list the values of two derived parameters obtained from the joint analysis of Planck and LSS data in Table 1.

## 6.2 Parameter space of neutrino mass: Viscous cosmology and other experiments

Recently, it has been shown that effective viscosity can resolve both  $\sigma_8$  and  $H_0$  tension simultaneously. Also, the phenomenon of neutrino oscillation has been observed by many experiments, which suggest that neutrinos are massive. We have already discussed how viscosity and massive neutrino affect the matter power spectrum  $P(k)$ . They have similar effects as both suppresses the  $P(k)$  at small length scales. Therefore, it is expected that constraints on the neutrino mass will be more stringent in the viscous framework of cosmology.

First, we did MCMC analysis of Planck and LSS combined dataset with six standard cosmology parameter and lightest neutrino mass  $m_0$ . We found that constraint on lightest neutrino mass is  $0.012 \text{ eV} \leq m_0 \leq 0.126 \text{ eV}$  for NH, whereas it is  $0 \leq m_0 \leq 0.119 \text{ eV}$  in the case of IH. This non-zero mass in the case of NH has arisen because we have not taken the viscous effect into account. We have also done the MCMC analysis in the effective viscosity framework with massive neutrino and found that the upper bound on  $m_0$  is  $0.084 \text{ eV}$  for NH and  $0.03 \text{ eV}$  for IH. Therefore, it is clear that bound on  $m_0$  is more stringent in the effective viscous framework as well as it rules out the notion of finding the non-zero mass. We also calculated the constraints on the sum of neutrino masses  $\sum m_\nu$  using the lightest neutrino mass obtained from our analysis and other parameters taken from [Capozzi et al. \(2016\)](#). We found

**Table 1.** Best-fit values of viscosity parameters, obtained from the Planck–LSS joint analyses. The best-fit values of two derived parameters  $\sigma_8$  and  $H_0$  are also listed

Parameters	1- $\sigma$ value	2- $\sigma$ value
$\tilde{\eta}$	$1.20^{+0.40}_{-1.00} \times 10^{-6}$	$1.20^{+1.00}_{-1.00} \times 10^{-6}$
$\tilde{\zeta}$	$1.32^{+0.50}_{-1.00} \times 10^{-6}$	$1.32^{+2.00}_{-1.00} \times 10^{-6}$
$\tilde{\zeta} = 0$		
$\tilde{\eta}$	$2.29^{+0.50}_{-0.60} \times 10^{-6}$	$2.29^{+1.00}_{-1.00} \times 10^{-6}$
$\tilde{\eta} = 0$		
$\tilde{\zeta}$	$2.46^{+0.50}_{-0.60} \times 10^{-6}$	$2.46^{+1.00}_{-1.00} \times 10^{-6}$
$H_0$ (km/s/Mpc)	$68.39 \pm 0.56$	$68.4^{+1.1}_{-1.1}$
$\sigma_8$	$0.754 \pm 0.011$	$0.754^{+0.022}_{-0.021}$

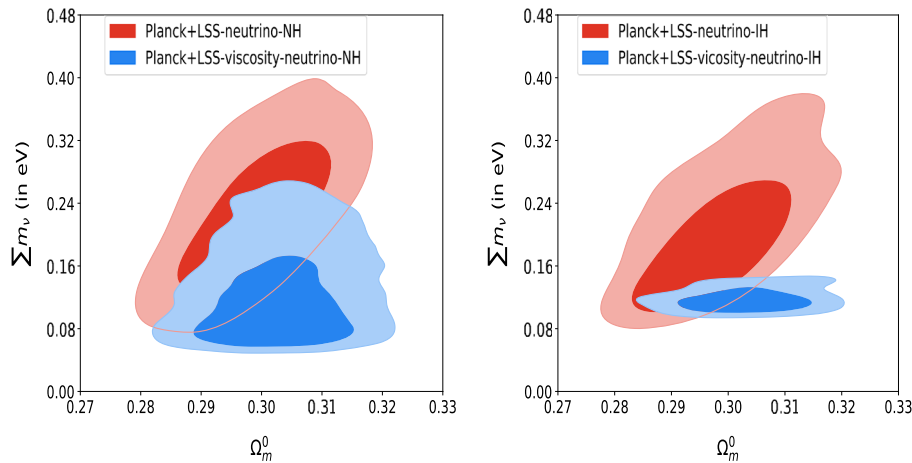


**Figure 5.** Constraint on the sum of neutrino masses  $\sum m_\nu$ , obtained from the analysis of combined Planck and LSS data decreases significantly over the inclusion of viscosity in CDM.

that the upper bound on  $\sum m_\nu$  changes from 0.396 eV and 0.378 eV to 0.267 eV and 0.146 eV for NH and IH respectively. This is shown in Fig. 5 which is taken from Anand *et al.* (2018).

## 7. Conclusion and discussion

The discrepancies in the value of  $\sigma_8$  and  $H_0$  have been reported extensively in the literature. At the same time, many theoretical models have also been proposed to explain these tensions. However, these proposals are plagued with several issues. For instance, the interaction between dark sectors, which have been proposed as a solution, is completely ad-hoc. Moreover, most of these proposals do not explain both the problems simultaneously.

On the other hand, we have considered the dissipative effects in the energy momentum tensor, which is characterized by the bulk and shear viscosities, in this analysis. These viscosities can be generated by the diffusive transport of momentum and by the constituent particles of the fluid. Alternatively, they can also be generated in an effective field theory treatment of large scale structure where small scale non-linearities are integrated to give rise to the large scale phenomenon. In this approach, UV and IR modes are coupled which can be described by an effective energy momentum tensor for imperfect fluid. We have found that either of the two viscosities or their combination affect the growth of linear overdensity which in turn changes the matter power spectrum at small length scales.

To quantify the amount of viscosity supported by the current observations, we have considered the viscosity coefficients as model parameters and performed MCMC analysis with Planck and LSS data. We found that the value of bulk and shear viscosity parameters are of the same order and have similar effects. The best-fit values for these viscosity parameters ( $\eta$  and  $\zeta$ ) are of the order of  $3 \times 10^2$  Pa s. It is interesting to note that the best-fit value of viscosity coefficients obtained resolve the conflict between Planck CMB and LSS observations, both in the  $\sigma_8 - \Omega_{m0}$  plane as well as the  $H_0 - \Omega_{m0}$  plane, simultaneously. We would like to highlight that the value of  $H_0$  inferred from Planck does not change significantly due to the viscosities, while the same obtained from LSS changes appreciably. The reason for this is the following:  $H_0$  is obtained from the baryon acoustic oscillation scale and depends on the value of  $\Omega_{m0}$ . The LSS experiments constrain  $\sigma_8$  and  $\Omega_{m0}$  jointly which gives a scope to accommodate lower  $\sigma_8$  by increasing  $\Omega_{m0}$ . However, in the case of Planck

data,  $\sigma_8$  is a derived parameter which comes down to a lower value, due to inclusion of viscosity, without affecting  $\Omega_{m0}$ . Therefore, in the case of  $\sigma_8$ , both Planck and LSS fitted values change on inclusion of viscosities, but for  $H_0$ , only the LSS value gets affected. We did not introduce any extra matter component to the  $\Lambda$ CDM cosmology.

As discussed earlier, inclusion of massive neutrinos does not solve both the problems simultaneously on its own but viscosity does. On the other hand, neutrino oscillation experiments have shown that the neutrinos are not massless. Thus, we consider the massive neutrinos in the viscous paradigm. Recall that the massive neutrinos have important property that they are relativistic in the early Universe and contribute to the radiation density while in the late time, when they turn non-relativistic, they contribute to the total matter density. The collisionless nature of the neutrinos, after they become non-relativistic, allow them to free-stream on scales  $k > k_{fs}$ . Hence, this will wash out the perturbations on length scales smaller than the characteristic scale  $k_{fs}$  leading to further suppression of power on small scales. Hence, in this viscous setup, stringent constraint on the mass of neutrinos can be put.

## References

- Abbott T. M. C. *et al.* 2017, Dark energy survey year 1 results: Cosmological constraints from galaxy clustering and weak lensing
- Ade P. A. R. *et al.* 2016a *Astron. Astrophys.*, 594, A13
- Ade P. A. R. *et al.* 2016b, *Astron. Astrophys.*, 594, A15
- Ade P. A. R. *et al.* 2014a, *Astron. Astrophys.*, 571, A20
- Ade P. A. R. *et al.* 2014b, *Astron. Astrophys.*, 571, A17
- Anand S., Chaubal P., Mazumdar A., Mohanty S. 2017, *JCAP*, 1711, 005
- Anand S., Chaubal P., Mazumdar A., Mohanty S., Parashari P. 2018, *JCAP*, 1805, 031
- Anderson L. *et al.* *MNRAS*, 441, 24
- Audren B., Lesgourgues J., Benabed K., Prunet S. 2013, *JCAP*, 1302, 001
- Aylor K. *et al.* 2017, A comparison of cosmological parameters determined from CMB temperature power spectra from the South pole telescope and the Planck satellite
- Bassett B. A., Hlozek R. 2009, *Baryon Acoustic Oscillations*, 2009
- Battye R. A., Charnock T., Moss A. 2015, *Phys. Rev.*, D91, 103508
- Battye R. A., Moss A. 2014, *Phys. Rev. Lett.*, 112, 051303
- Blas D., Lesgourgues J., Tram T. 2011, *JCAP*, 1107, 034
- Blas D., Floerchinger S., Garny M., Tetradis N., Wiedemann U. A. 2015, *JCAP*, 1511, 049

- Brevik I., Grøn Ø., de Haro J., Odintsov S. D., Saridakis E. N. 2017, Viscous cosmology for early- and late-time Universe
- Capozzi F., Lisi E., Marrone A., Montanino D., Palazzo A. 2016, Nucl. Phys., B908, 218
- Costanzi M., Villaescusa-Navarro F., Viel M., Xia J.-Q., Borgani S., Castorina E., Sefusatti E. 2013, JCAP, 1312, 012
- Font-Ribera A. *et al.* 2014, JCAP, 1405, 027
- Heymans C. *et al.* 2013, MNRAS, 432, 2433
- Hinshaw G. *et al.* 2013 Astrophys. J. Suppl., 208, 19
- Joudaki S. *et al.* 2017, MNRAS, 471, 1259
- Kilbinger M. *et al.* 2013, MNRAS, 430, 2200
- Ko P., Tang Y. 2016, Phys. Lett., B762, 462
- Ko P., Tang Y. 2017, Phys. Lett., B768, 12
- Ko P., Nagata N., Tang Y. 2017, Hidden charged dark matter and chiral dark radiation
- Kunz M., Nesseris S., Sawicki I. 2016, Phys. Rev., D94, 023510
- Lambiase G., Mohanty S., Narang A., Parashari P. 2018, Testing dark energy models in the light of  $\sigma_8$  tension
- Lesgourgues J., Tram T. 2011, JCAP, 1109, 032
- Lin W., Ishak M. 2017 Phys. Rev., D96, 023532
- Ma C.-P., Bertschinger E. 1995, Astrophys. J., 455, 7
- Macaulay E., Wehus I. K., Eriksen H. K. 2013, Phys. Rev. Lett., 111, 161301
- MacCrann N., Zuntz J., Bridle S., Jain B., Becker M. R. 2015, MNRAS, 451, 2877
- Pan Z., Knox L., White M. 2014, MNRAS, 445, 2941
- Park C.-G., Ratra B. 2018, Observational constraints on the tilted flat- $\Lambda$ CDM and the untilted non-flat  $\Lambda$ CDM dynamical dark energy inflation parameterizations
- Perlmutter S. *et al.* 1997, Astrophys. J., 483, 565
- Perlmutter S. *et al.* 1999, Astrophys. J., 517, 565
- Pourtsidou A., Tram T. 2016, Phys. Rev., D94, 043518
- Press W. H., Schechter P. 1974, Astrophys. J., 187, 425
- Raveri M. 2016, Phys. Rev., D93, 043522
- Riemer-Sørensen S., Parkinson D., Davis T. M. 2014, Phys. Rev., D89, 103505
- Riess A. G. *et al.* 1998, Astron. J., 116, 1009
- Rubin V. C., Ford W K. Jr. 1970, Astrophys. J., 159, 379
- Salvatelli V., Said N., Bruni M., Melchiorri A., Wands D. 2014, Phys. Rev. Lett., 113, 181301
- Schaffer K. K. *et al.* Astrophys. J., 743, 90
- Sheth R. K., Tormen G. 1999, MNRAS, 308, 119
- Thomas D. B., Kopp M., Skordis C. 2016, Astrophys. J., 830, 155
- Tinker J. L., Kravtsov A. V., Klypin A., Abazajian K., Warren M. S., Yepes G., Gottlober S., Holz D. E. 2008, Astrophys. J., 688, 709
- Troxel M. A. *et al.* 2017, Dark energy survey year 1 results: Cosmological constraints from cosmic shear
- van Engelen A. *et al.* 2012, Astrophys. J., 756, 142
- Velten H., Carami T. R. P., Fabris J. C., Casarini L., Batista R. C. 2014, Phys. Rev., D90, 123526
- Vikhlinin A. *et al.* 2009, Astrophys. J., 692, 1060
- Weinberg S. 1972, Gravitation and Cosmology, John Wiley and Sons, New York, pp. 55–57
- Wyman M., Rudd D. H., Vanderveld R. Ali, Hu W. 2014, Phys. Rev. Lett., 112, 051302
- Yang W., Xu L. 2014, Phys. Rev., D89, 083517
- Zwicky F. 1933, Helv. Phys. Acta, 6, 110 (Gen. Relativ. Gravit., 41, 207 (2009))